Journal of Multidisciplinary Engineering Science and Technology (JMEST)
ISSN: 2458-9403
Vol. 4 Issue 9, September - 2017

Effect Of Thickness On Structural, Optical And Sensing Properties Of SnS Thin Films Prepared By Ultrasonic Nebulizer Method

Salah. Q. Haza'a , Hiba R. Shaker
Department of Physics, College of Education, Al- Mustansiriyah University

***Abstract*—Thin Film of tin sulfide with different thickness (100, 250, 450, 600) nm have been prepared on pre-heated glass substrates up to (430 ^{o}C) by Ultrasonic Nebulizer Deposition (UND). The effect of thickness on the structural, optical, and gas sensing properties of films has been investigated. The results of the XRD show that the film which deposited with thickness (100 and 250) nm exhibit only SnS phase with (111) orientation, and with thickness (450 and 600) nm crystallized in the mixed phase SnS and Sn_2S_3 depending upon the films thickness. Atomic force measurement showed the grain size increase with thickness in the range of (76.08 - 105.67 nm). The optical properties of the films have been studied over a wavelength (370-1100) nm. The calculated optical energy band gap values were between 1.3 and 2.4 eV, depending on the film thickness and in which phase crystallized. The effect of thickness and operating temperature on performance of the sensor material has been investigated to choice optimum thickness and temperature for each ethanol and ammonia gases. The films with 600 nm thickness showed high response and excellent sensitivity for ethanol and ammonia gases at low temperature (140,110) ^{o}C and high temperature (380,240) ^{o}C respectively.**

Keywords—SnS, Thin Films, Ultrasonic Nebulizer Technique, Gas Sensors.

Introduction:

Tin sulfide (SnS) belongs to IV-VI compound semiconductor materials with p-type electrical conductivity [1]. Its optical band gap ranges in between 1.2 - 1.7 eV. It has an orthorhombic crystal structure with lattice parameters a = 0.4329 nm, b = 1.1193 nm, c = 0.398nm, where Sn & S are bonded by weak Van Der Waal's force [2]. The constituent elements of tin and sulfur are nontoxic and abundant in nature leading to development of devices that are environmentally safe and have public acceptability. Variations in the properties and diversity in the applications of thin films can be achieved through the use of different deposition methods, deposition parameters and impurity ions [3]. It will be also wise to mention here that pure SnS single phase is always accompanied by trace amount of SnS2 phase and so the band gap variation can be attributed to this fact [4]. SnS thin films have been synthesized by different techniques such as the chemical bath deposition CBD [5] thermal evaporation [6] chemical bath deposition dip coating and SILAR[7], spray ultrasonic[8] and sputtering techniques[9] In this work, we investigated the effect of film thickness on the structural, optical and sensing properties of SnS films prepared by Ultrasonic Nebulizer technique.

Recently a sufficient amount of work has been reported on tin oxide. But no work has been reported on the SnS to detect ammonia gas and ethanol vapours. We report here the use of SnS thin film prepared by Ultrasonic Nebulizer method as a gas sensors to sense ammonia gas and ethanol vapor's and to study the effect of thickness and operating temperature on structural, optical and gas sensing properties of SnS thin film .

Experimental Details

Tin sulfide films were deposited onto preheated glass slides(430^{o}C) with different thickness by Ultrasonic Nebulizer Deposition (UND) technique. Tin Chloride salt ($SnCl_2 \cdot 2H_2O$, 234.644 g/mol (99.98%) pure BDH Chemical Ltd Pool England) and thiourea($CS(NH_2)_2$) 76.12g/mol ,99% pure, BDH Chemical Ltd Pool England) were dissolved in distilled water. The precursor solution of tin sulfide films was prepared by mixed aqueous solution (1:1)of Tin Chloride salt (0.2 M) and aqueous solution of thiourea (0.2 M) to make a 0.2 M solution of total metal content. The resulting solution was sprayed onto heated glass substrates using an ultrasonic nebulizer system (Sonics), which transformed the liquid to a steam. In order to get good quality films and complete combustion all the deposition parameters such as the distance between the substrate and the nozzle, gas flow rate, deposition temperature, and the concentration of the solutions were optimized.

Film thickness (t) measured by weight difference method and optical interferometer method. The optical method was based on interference of He-Ne laser light beam reflected from film surface and substrate bottom by using the known formula:

$$t = \frac{\Delta x}{x} \times \frac{\lambda}{2} \quad \ldots\ldots \quad 1$$

Where x is fringe width, Δx is the distance between two fringes and λ is wavelength of laser light(632.8 nm).

The structural properties of the films were characterized by X-ray diffraction (XRD) using PHILIPS PW 1840 diffractometer with Cu Kα radiation (λ= 1.5406 Å) operated at 40 kV and 30 mA. All samples were scanned in the range (20° to 70°) with a scan speed of 5°/min. Surface studies of the samples were done with the help of atomic force microscopy (AFM) type (SPM-AA3000 contact mode spectrometer, Angstrom)

Optical transmission and absorption spectra of the films were recorded in the wavelength range of (370- 1100) nm using UV–VIS– NIR spectrophotometer (type Shimadzu).

The gas sensing properties were evaluated at various operating temperatures, from 60 to 410℃, by measuring the changes of resistance of the sensor in air and in the gas (ethanol and ammonia gas). The sensitivity in the experiment was defined as S=Ra/Rg where Ra is the sample resistance measured in the ambient environment while Rg is that under the test gas [10,11].

Results and discussion

Figure (1) shows XRD pattern of films deposited at different thickness (100, 250,450 and 600 nm). Films deposited with thickness 100 nm and 250 nm , had predominantly SnS phase orientated along (111) plane at 2θ=31.7° the peak positions matched with those reported in JCPDS card No 39-0354,. Another peaks at 2θ =26.6° along (111) observed at higher thickness (450 and600 nm) indicated of Sn_2S_3 phase. The average crystallite size (G) of the films calculated from the peak (111) for SnS phase using the following relation (Debye-Scherer formula)[12]:

$$G = \frac{0.9\,\lambda}{\beta\cos\theta} \quad \ldots\ldots\ldots \quad 1$$

Where, λ is the wavelength of x-rays which is equal to 1.5406 Å, β is the full width at half maximum (FWHM) measured in radians and θ is the Bragg angle. The result showed that the film at 250 nm having better crystallinity with single phase SnS as shown in Table (1).

Using d values for SnS phase for the orthorhombic systems, lattice parameters a, b and c are calculated with the help of eq. (2) and listed in Table (1).The result showed that the all values are agreement with standard JCPDS [13]:

$$\frac{1}{d^2} = \frac{h^2}{a^2} + \frac{k^2}{b^2} + \frac{l^2}{c^2} \qquad \text{----------2}$$

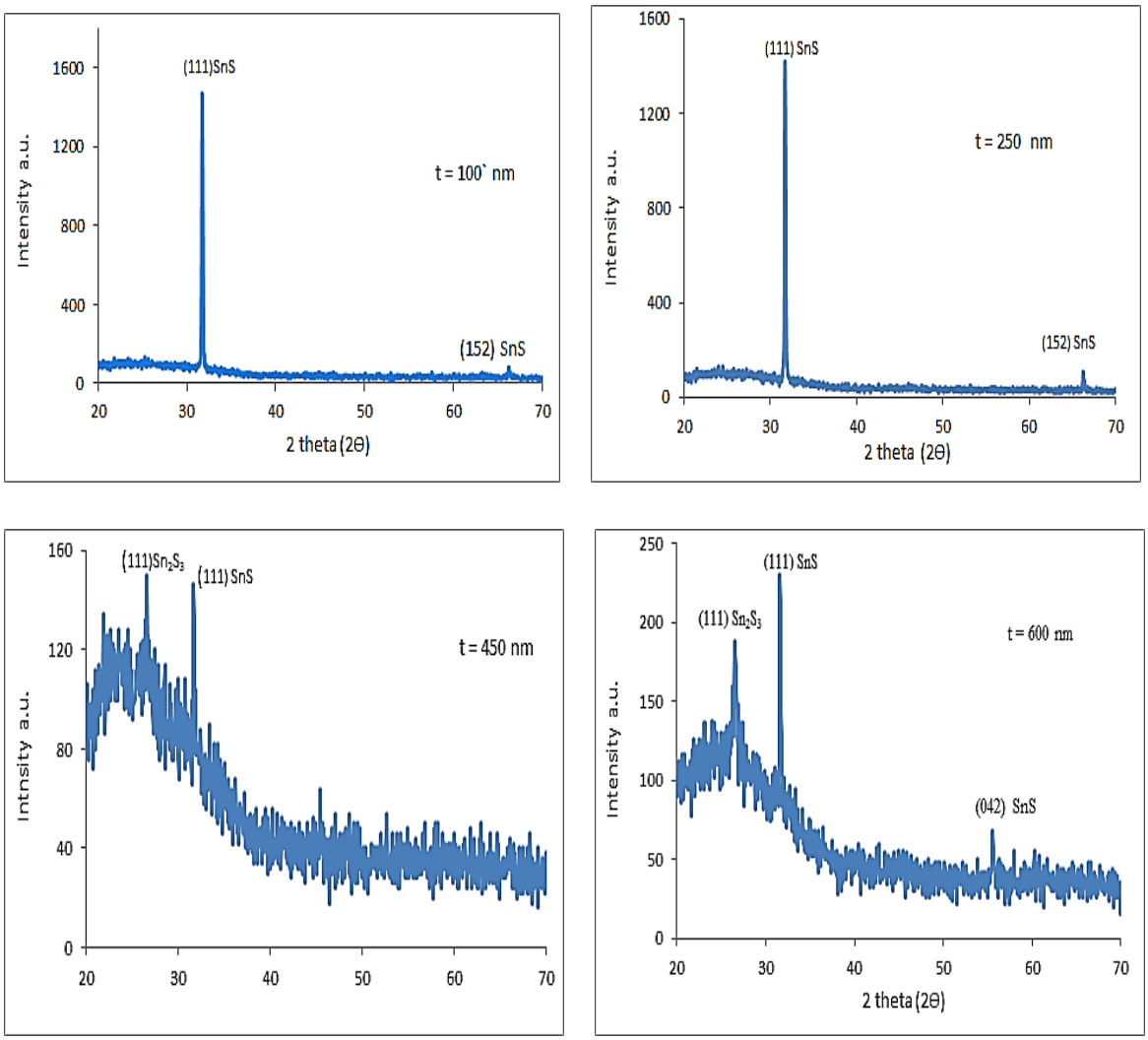

Figure (1) XRD of SnS Thin films at at different thickness

Table (1) shown the result from the X-Ray Diffraction measurement for SnS different thickness.

Sample		ASTM	SnS t=100nm	SnS t=250nm	SnS t=450nm	SnS t=600nm
2θ (deg)	(111)	31.35	31.7542	31.4915	31.7556	31.6471
$d_{(hkl)}$ (Å)	(111)	2.835	2.81568	2.8386	2.81556	2.82497
FWHM	(111)	-	0.1406	0.1334	0.3088	0.2064
Lattice Constants	$a_\circ$(Å)	3. 98	3.2435	3.2454	3.2473	3.2400
	$b_\circ$(Å)	11.192	11.264	11.262	11.299	11.262
	$c_\circ$(Å)	5.206	5.0204	4.141	5.833	4.152
G (nm)	(111)	-	58.77	61.9	26.75	40.03

Atomic force microscopy (AFM)

The figure (3) shown the **images** (AFM) of SnS thin films for different thickness on the glass substrate at temperature (430^{o}c), the Table (2) shown the Root mean square (RMS), Roughness and Grain size

different with films thickness. The Grain size range values between (76.08-105.67 nm) these values indicate of increase surface roughness comfort into increase the size of all crystalline [14].

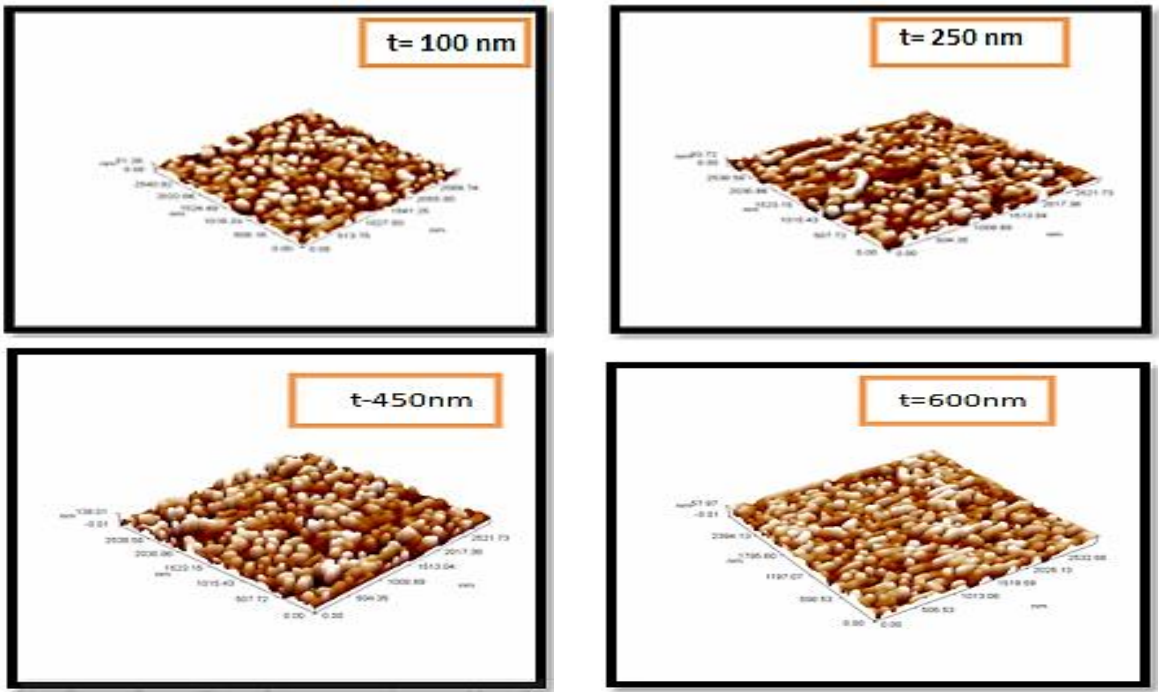

Figure (3) AFM images for SnS films at different thickness

Table (2): Shown the result from the (AFM) of SnS different thickness.

SnS (nm)	Roughness (nm)	RMS (nm)	Grain size (nm)
100	12 .1	14	76.08
250	20.1	23.4	95.88
450	34.8	40.1	99.15
600	11.4	13.8	105.67

Optical properties:

The optical properties of all films with different thicknesses (100, 250, 450 and 600 nm) have been determined by using transmittance (T) and absorbance (A) spectrum in the region (370-1100nm). Figure (3) and figure(4) shown that the transparency decreases and absorbance increases as the thickness increase may due to thickness or to absorption coefficient . The absorption coefficient (α) which is a function of the photon energy ($h\nu$) is calculated from the optical transmittance spectra results using the following equation [15]:

$$\alpha = (1/t) \ln (1/T) \quad \ldots\ldots\ldots \quad 4$$

All the films as shown in Figure(5) had high absorption coefficient, ($\alpha > 10^5$ cm^{-1}) above the fundamental absorption edge, indicates the existence allowed transitions, and the absorption coefficient increase as the thickness increase.

The optical band gap was calculated using following [15]:

$$\alpha h\upsilon = B(h\upsilon - E_g)^r \quad \ldots\ldots\ldots \quad 5$$

Where $h\upsilon$ is the photon energy, E_g is the optical band gap, B is a constant and r is 1/2, 3/2, 2 or 3 for direct allowed, direct forbidden, indirect allowed and indirect forbidden transitions, respectively. A

satisfactory linear fit is obtained for $(\alpha h\upsilon)^2$ vs. $h\upsilon$, indicating the presence of direct allowed transition for thin films. The intercept on the energy axis, as shown in Figures (6), gives the band gap E_g of the material and listed in Table (2).

The results showed that the optical band gap decreased with increase in thickness up to 250 nm and reached 1.3 eV, then increased with increasing films thickness and reached 2.4 eV for the film with t=600nm. This large band gap value may be due to presence Sn_2S_3 (Eg = 2.0 eV) in SnS thin films [16]. Poor crystallinity of the films may also lead to higher optical band gap. These values of optical band gap is comparable with the reported value for SnS thin films [17,18,19].

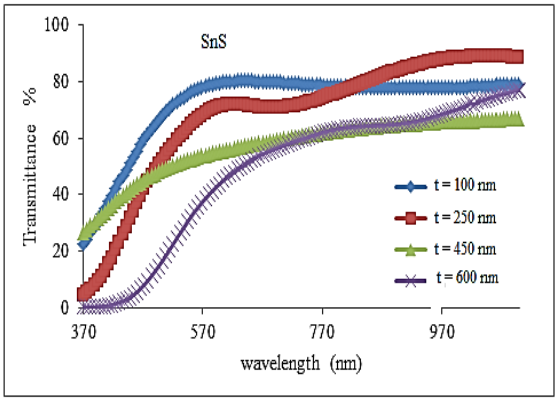

Figure (3) transmittance as a function of wavelength at different thickness

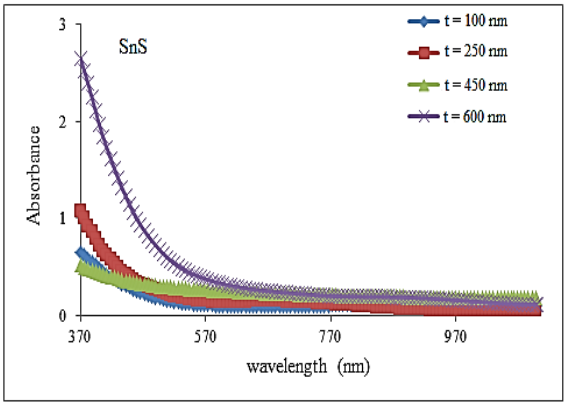

Figure (4) absorbance as a function of wavelength at different thickness

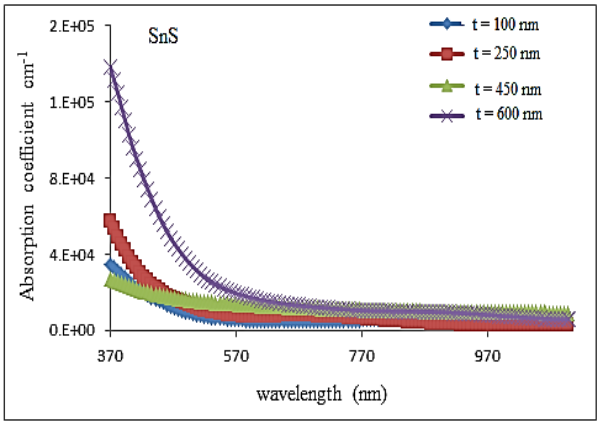

Figure (5): absorption coefficient as a function of wavelength at different thickness

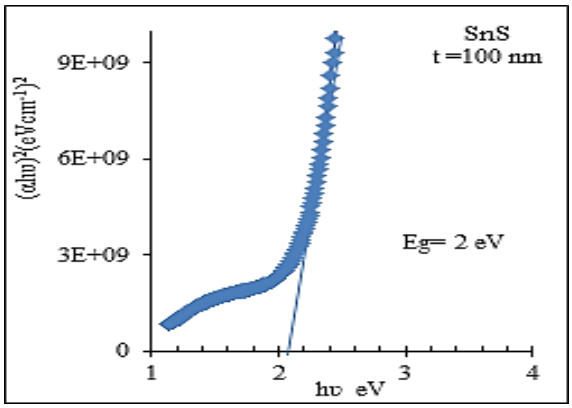

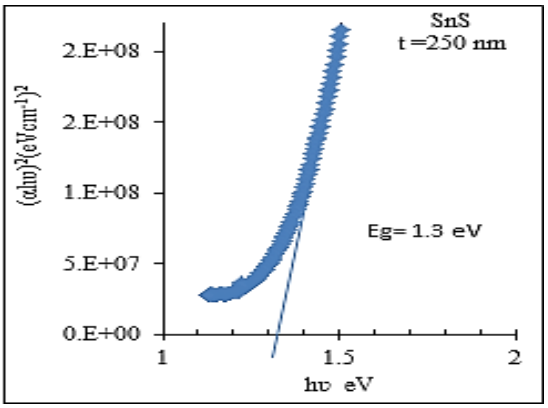

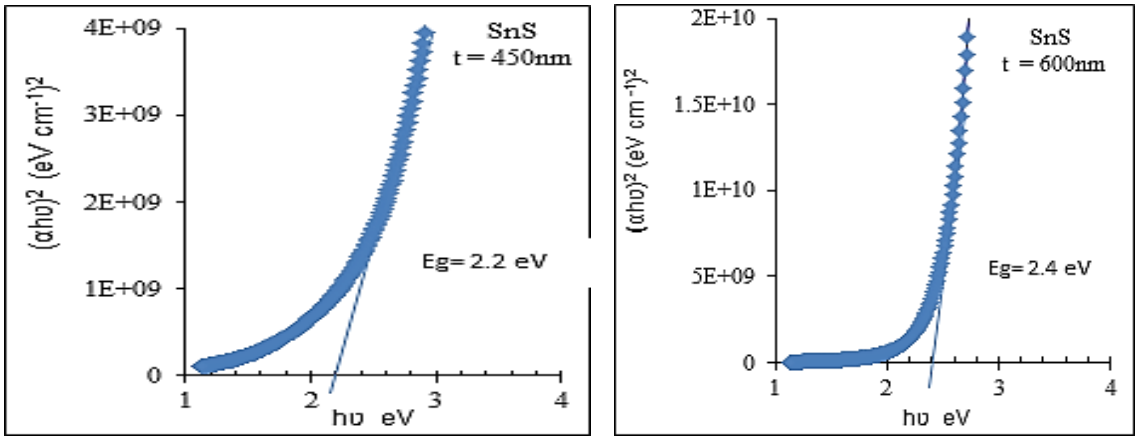

Figure (6) $(\alpha h\nu)^2$ versus photon energy for SnS films with different thickness.

Table (3) optical band gap for SnS films with different thickness.

Thickness	100nm	250nm	450nm	600nm
E_g	2.0 eV	1.3 eV	2.2 eV	2.4 eV

Figure (7) and figure (8) show the variation of sensitivity vs. operating temperature at different thickness in the presence of 20 ppm ethanol gas and ammonia gas respectively. This variation (increases and decrease) in the sensitivity indicates the adsorption and desorption phenomenon of the gases due to optimum number of misfits on the surface, porosity, largest surface area or present Sn_2S_3 phase. Maximum peak values are seen at certain temperatures called optimal temperature depended on the thickness and the type of the gas, and all films has two optimum temperature (T1and T2)this is may be due to existence two activation energy. At the optimal temperature, the activation energy may be enough to complete the chemical reaction.

Also, as seen from a plot of sensitivity against the operating temperature, the sensitivity depending on the thickness the thicker film(600 nm) has higher sensitivity and on the type of the gas and sensitivity of the films for ethanol gas is higher than that for ammonia gas , as shown in Table(4).

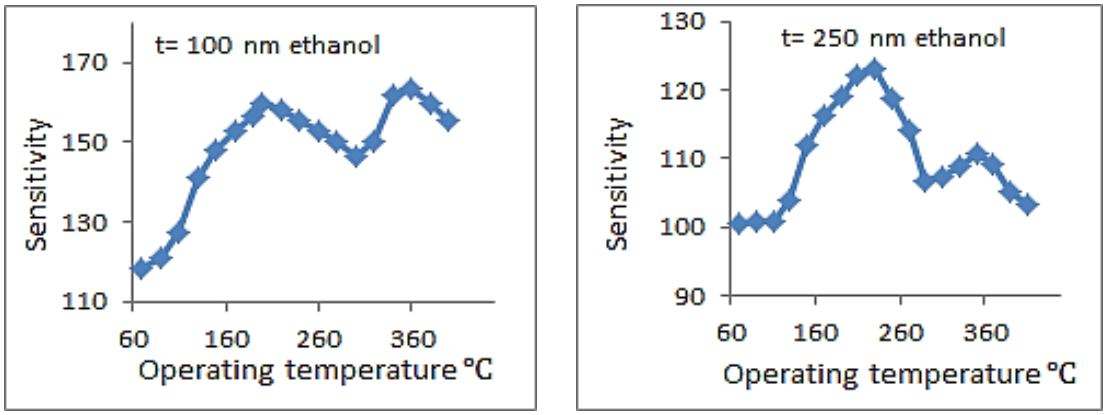

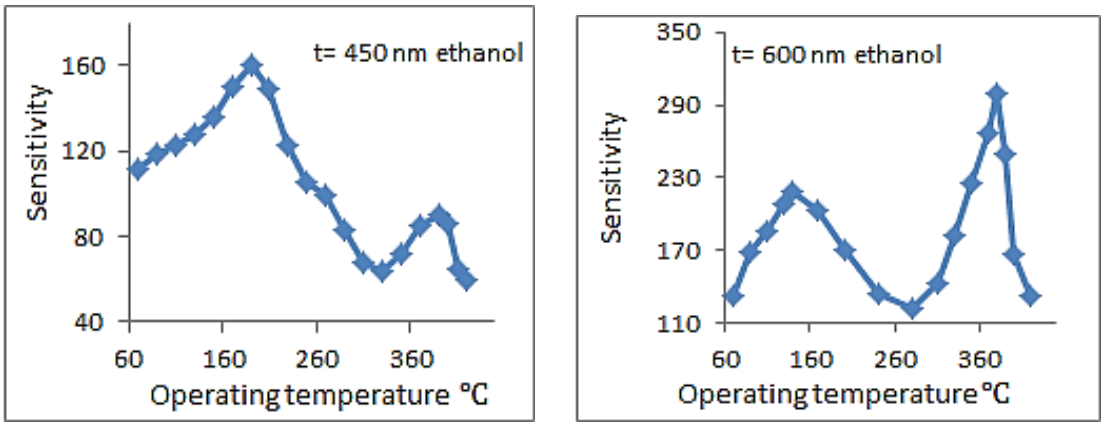

Figure (7) Variation of sensitivity with temperature of SnS thin film for 20 ppm ethanol at different thickness

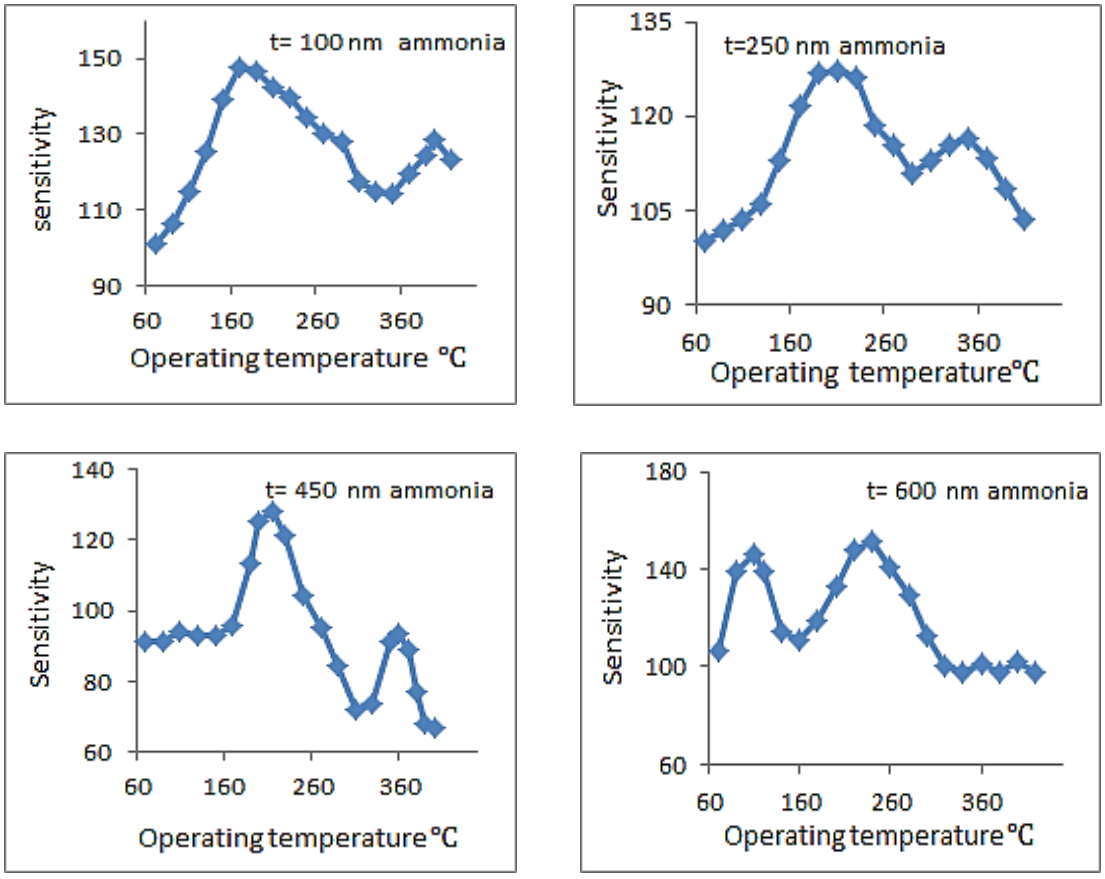

Figure (8) Variation of sensitivity with temperature of SnS thin film for 20 ppm ammonia at different thickness

Table (4) optimal temperature and high Sensitivity with thickness for ethanol ammonia gases

Gas	Thickness nm	T1 ℃	Sensitivity 1	T2 ℃	Sensitivity 2
ethanol	100	160	160	360	162
ethanol	250	230	122	350	111
ethanol	450	190	160	390	90
ethanol	600	140	218	380	300
ammonia	100	170	148	400	129
ammonia	250	190	127	350	117
ammonia	450	215	128	360	93

ammonia	600	110	146	240	152

Conclusion

SnS thin films were successfully deposited by Ultrasonic Nebulizer Deposition (UND) onto glass substrates at temperature (430^{o}c). The XRD spectrum shows that all films are polycrystalline. Pure SnS can prepare by Ultrasonic Nebulizer Deposition (UND) with thinner thickness. According to AFM results the Grain size range values between (76.08-105.67 nm), the direct energy band gaps of the films were determined as (1.3 -2.4 eV), all the films has two operating temperature, maximum sensitivity obtained thickness 600 nm, the sensitivity of thin films to ethanol is higher than ammonia and it can used as gas sensors .

Refrence

1- H. M. Pathan, C. D. Lokhande, "Deposition of metal chalcogenide thin films by successive ionic layer and adsorption and reaction (SILAR) method", Bull of Materials Science, 27(2),(2004) pp. 85-111.
2- B. Ghosh, R. Roy, S. Chowdhury, P. Banerjee, S. Das, "Synthesis of SnS thin films via galvanostatic electrodeposition and fabrication of CdS/SnS heterostructure for photovoltaic applications", Applied Surface Science, 256 (2010) pp. 4328–4333.
3- J. C. Osuwa and J. Ugochukwu," Effects of aluminum and manganese impurity concentrations on optoelectronic properties of thin films of Tin Sulfide (SnS) using CBD method", IOSR Journal of Environmental Science, Toxicology And Food Technology (IOSR-JESTFT), 5, Issue 3 (Jul. - Aug. 2013) PP 32-36.
4- B. Ghosh, M. Das, P. Banerjee, S. Das, "Fabrication of vacuum-evaporated SnS/CdS heterojunction for PV applications", Solar Energy Materials and Solar Cells, 92 (9), (2008) pp.1099-1104.
5- A. M. Patil, A. C. Lokhande, P. A. Shinde, H. D. Shelke, C. D. Lokhande , "Electrochemical supercapacitor properties of SnS thin films deposited by low-cost chemical bath deposition route", International Journal of Engineering Research and Technology. ISSN 0974-3154 Volume 10, Number 1 (2017), PP 914-922
6- A. A. Shehab, N. A. AL-Hamadni, D. M. A. Latif, "Effect of annealing temperature on the Photodetector characteristic of SnS /Si heterojunction", Journal of Multidisciplinary Engineering Science Studies (JMESS), 2 Issue 9, (September – 2016) pp.892-897.
7- S. H. Chaki, M. D. Chaudhary, and M. P. Deshpande, "SnS thin films deposited by chemical bath deposition, dip coating and SILAR techniques", Journal of Semiconductors, 37(5),(May2016) pp. 0530011- 0530019.
8- I. B. Kherchachi ,A. Attaf, H. Saidi, A. Bouhdjer, H. Bendjedidi, Y. Benkhetta, and R. Azizi, "Structural, optical and electrical properties of Sn_xS_y thin films grown by spray ultrasonic", Journal of Semiconductors, 37(3),(March2016) pp. 0320011- 0320016.
9- R. E. Banai, H. Lee, S. Zlotnikov, et al., "Phase identification of RF-sputtered SnS thin films using rietveld analysis of X-ray diffraction patterns", IEEE 39th Photovoltaic Specialists Conference(PVSC),Tampa, FL,(2013) pp.2562-2566
10- S. Q. Hazaa, M. Th. Mansor, N. A. Al-Hamadani," Undoped and cobalt doped ZnO thin films ethanol gas sensors", International Journal of Latest Research in Engineering and Technology (IJLRET), 2 - Issue 8 ,(August 2016) pp. 1-5.

11- S. Q. Hazaa,S. A. Salman, S. J. Abbas, ”ZnO:Sn thin films gas sensor for detection of ethanol”, International Journal of Advancement In Engineering Technology, Management and Applied Science (IJAETMAS),3Issue 11(November - 2016) pp. 72-76 .
12- S. Haza'a, “Effect of post annealing on structural and optical properties of SnO2 thin Films deposited by Dc magnetron sputtering”, IOSR Journal of Applied Physics ,(IOSR-JAP), 7,Issue 1 (Jan - Feb – 2015) pp. 59-63.
13- A. A. Shehab. , N. A. AL-Hamadni., D. M .A. Latif, Effect of annealing temperature on structure properties of SnS thin films, Physical Chemistry An Indian Journal, 9(7), (2014) pp.255-159.
14- P. Sagar, M. Kumar, R. M. Mehra, "Electrical and optical properties of sol-gel derived ZnO:Al thin films", Materials Science-Poland, 23(3),(2005) pp.685-696.
15- N. A. Al-Hamadani, A. A. Salih," Preparation of nanocrystalline copper doped CdS thin films by spray pyrolysis method", Diyala Journal for pure Sciences, 8(3),(July 2012) pp. 285-295.
16- S. Cheng, G. Conibeer, “Physical properties of very thin SnS films deposited by thermal evaporation”, Thin Solid Films, 520, ISSUE 2, 1 (November 2011) pp. 837-841.
17- B. A. Hasan, and I. H. Shallal, “Structural and optical properties of SnS thin films Journal of Nanotechnology & Advanced Materials 2(2), (2014)pp. 43-49.
18- N. R. Mathews, Hiran B. M. Anaya, M. A. Cortes-Jacome, C.Angeles-Chavez, J. A. Toledo Antoniob, “Tin sulfide thin films by pulse electro deposition: structural, morphological, and optical properties”, Journal of The Electrochemical Society, 157(2010)pp. H337-H341.
19- H. Kafashan ,Z. Balak,”Preparation and characterization of electrodeposited SnS:In thin films: Effect of In dopant”, Spectrochimica Acta Part A: Molecular and Biomolecular Spectroscopy, 184(5),(September 2017) pp.151-162.